Explicitly correlated treatment of H2NSi and H2SiN radicals: Electronic structure calculations and rovibrational spectra

D. Lauvergnat, M. L. Senent, L. Jutier, and M. Hochlaf

Citation: J. Chem. Phys. **135**, 074301 (2011); doi: 10.1063/1.3624563
View online: http://dx.doi.org/10.1063/1.3624563
View Table of Contents: http://jcp.aip.org/resource/1/JCPSA6/v135/i7
Published by the American Institute of Physics.

Explicitly correlated treatment of H_2NSi and H_2SiN radicals: Electronic structure calculations and rovibrational spectra

D. Lauvergnat,[1,a)] M. L. Senent,[2] L. Jutier,[3] and M. Hochlaf[3,b)]
[1]*CNRS, Laboratoire de Chimie Physique, Bât. 349, UMR 8000, Orsay, F-91405; Université Paris-Sud, Orsay, F-91405, France*
[2]*Departamento de Química y Física Teóricas, Instituto de Estructura de la Materia, IEM-C.S.I.C., Serrano 121, Madrid 28006, Spain*
[3]*Laboratoire de Modélisation et Simulation Multi Echelle, Université Paris-Est, MSME UMR 8208 CNRS, 5 boulevard Descartes, 77454 Marne-la-Vallée, France*

(Received 6 April 2011; accepted 7 July 2011; published online 15 August 2011)

Various *ab initio* methods are used to compute the six dimensional potential energy surfaces (6D-PESs) of the ground states of the H_2NSi and H_2SiN radicals. They include standard coupled cluster (RCCSD(T)) techniques and the newly developed explicitly correlated RCCSD(T)-F12 methods. For H_2NSi, the explicitly correlated techniques are viewed to provide data as accurate as the standard coupled cluster techniques, whereas small differences are noticed for H_2SiN. These PESs are found to be very flat along the out-of-plane and some in-plane bending coordinates. Then, the analytic representations of these PESs are used to solve the nuclear motions by standard perturbation theory and variational calculations. For both isomers, a set of accurate spectroscopic parameters and the vibrational spectrum up to 4000 cm^{-1} are predicted. In particular, the analysis of our results shows the occurrence of anharmonic resonances for H_2SiN even at low energies. © *2011 American Institute of Physics*. [doi:10.1063/1.3624563]

I. INTRODUCTION

The general interest on silicon-nitrogen compounds resides on their rich and complex chemistry, their importance on several media, and their wide applications. Indeed, silicon atom and ions play crucial roles in the chemistry of the low earth atmosphere (e.g., ionosphere), in interstellar media, and in plasma physics.[1–9] Moreover, the gas-phase ion-molecule reactions of silicon ion Si^+ with ammonia and small amines, or reactions of ammonia on Si surfaces or Si clusters,[10,11] are possible pathways toward a wide variety of $Si_xH_yN_z$ compounds. From the point of view of applications, silicon nitride containing materials, which present specific thermal and elasticity properties, are popular insulating layer in silicon-based electronics and silicon nitride cantilevers.[12–15] They are also the sensing parts of atomic force microscopes. Finally, Chen *et al.*[16] showed that $Si_xH_yN_z$ compounds may act as an effective reagent to convert the reactive and toxic NO into a benign gas N_2 in several NO-producing combustion systems.

The present theoretical contribution treats fully the rovibrational spectroscopy of the H_2NSi and H_2SiN radicals. Recently, some of us characterized the stable isomers of H_2NSi by means of the state-of-the-art mono and multiconfigurational *ab initio* approaches and extended basis sets.[17] Our calculations confirmed the existence of three stable isomers (see Figure 1): H_2NSi (denoted as I), *trans*-HSiNH (II), and H_2SiN (III).

H_2NSi represents the most stable form, followed by the *trans* form and the H_2SiN isomer lying at 0.68 eV and 1.88 eV, respectively. We also showed that the energy barriers for intramolecular isomerisation and the lowest dissociation energies (deprotonation channels) are higher than 1 eV. Hence, each isomer can be treated separately for its spectroscopy.

Experimentally, H_2NSi species and related ions were identified in the mass spectrometric investigations of Goldberg *et al.*,[18] using the flowing afterglow selected ion flow tube technique,[19] and after reactive collisions between N and SiH_4,[20,21] and between silicon cation, Si^+, and ammonia and small amines.[22] These identifications were supported by density functional theory and *ab initio* calculations.[18,20,21,23–27]

In the present study, we map the six-dimensional potential energy surfaces (6D-PESs) of the formaldehyde-like isomers (i.e., H_2NSi and H_2SiN) in their electronic ground state using the standard coupled cluster approach (RCCSD(T)/aug-cc-pV5Z) and using the newly implemented explicitly correlated RCCSD(T)-F12a/b techniques. This work does not treat the *trans*-HSiNH form because of the multiconfigurational nature of its wavefunction in contrast to the monoconfigurational nature of two others.[17] Then, our 6D-PESs are incorporated into perturbative and variational treatments to solve the nuclear motion problem. We derived, hence, accurate spectroscopic terms and the full rovibrational spectra of these radicals. Our calculations reveal the presence of some strong anharmonic resonances between the vibrational levels even at low energies, thus makes difficult their assignments by vibrational quantum numbers. We will also discuss the applicability and the validity of the available theoretical approaches for the accurate treatment of the rovibrational

a)Electronic mail: david.lauvergnat@lcp.u-psud.fr.
b)Author to whom correspondence should be addressed. Electronic mail: hochlaf@univ-mlv.fr. Telephone: +33 1 60 95 73 19. Fax: +33 1 60 95 73 20.

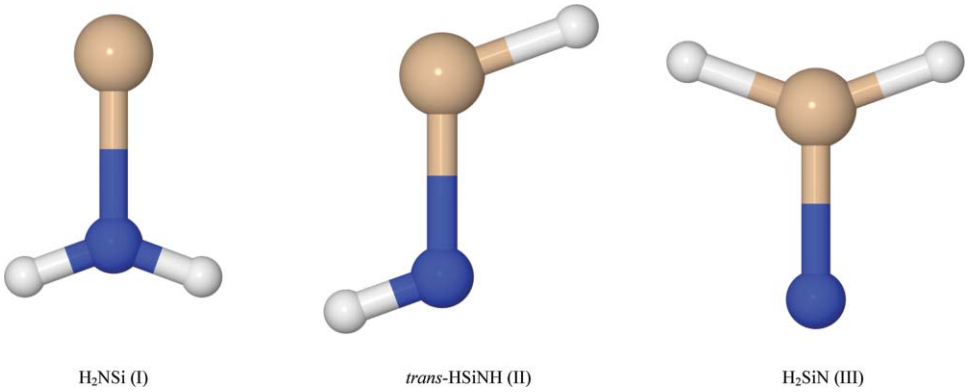

FIG. 1. Scheme of the three isomers of H_2SiN.

spectroscopy of such molecular systems. Especially, we will check the possibility of (R)CCSD(T)-F12a/b methods in taking into account anharmonic effects through the accurate description of the floppiness of the PESs along some internal coordinates such as the in-plane and out-of-plane angles and when they are strongly coupled together.

II. GENERATION OF THE 6D-POTENTIAL ENERGY SURFACES

A. Electronic structure calculations

All electronic calculations were done using the MOLPRO program suite[28] in the C_1 point group. We performed electronic computations using the coupled cluster approach with perturbative treatment of triple excitations (RCCSD(T))[29,30] and the newly developed and implemented RCCSD(T)-F12 technique (using both F12a and F12b approximations)[31,32] as detailed in Ref. 33. For the description of silicon, nitrogen, and hydrogen atoms, we employed the aug-cc-pV5Z basis set by Dunning and co-workers[34,35] for the standard coupled cluster calculations. For the RCCSD(T)-F12 computations, the cc-pVTZ-F12 explicitly correlated basis set by Peterson and co-workers[33] in connection with the corresponding auxiliary basis sets and density fitting functions,[36–38] are used. For a single point calculation, a strong reduction on the cost of computations, both CPU time and disk used, are observed (one to two orders of magnitude) when using RCCSD(T)-F12 instead of RCCSD(T). This result, which shows the applicability of F12 methods for large systems, was explicitly discussed previously.[39–41] Apart from systematic shifts in total energies over the grid when using RCCSD(T)-F12a or RCCSD(T)-F12b, both approximations lead to very close data. In the following, we will discuss without distinguishing the RCCSD(T)-F12a or RCCSD(T)-F12b results except when explicitly stated.

Recently, Lee and co-workers[42] performed benchmark calculations on several molecular systems where core-correlation, scalar relativity, higher order electron correlation, and one-particle basis set extrapolation effects were included. For HN_2^+ cation, these authors found a good agreement with the previously computed data of Brites and Hochlaf who have not considered such effects. Such agreement is surely not fortuitous since the F12 methods are proved to describe efficiently electron correlation. For both isomers, we performed geometry optimizations and harmonic frequencies calculations using standard RCCSD(T) method with and/or without core-valence correlation and/or with relativistic corrections to attest on the quality of the present methodology. We used the following basis sets: aug-cc-pVTZ, aug-cc-pCVTZ (within the core zero and within the frozen core approximations for core-valence correlation), aug-cc-pVXZ-DK (X = T,Q), and aug-cc-pV(T+d)Z. These corresponding results are detailed in the supplementary material.[43] All these results show that core-correlation corrections are for the Si–N distances about 0.02 bohr and about 0.01 bohr for the Si–H bond length. Scalar relativistic corrections are actually negligible, while additional tight *d*-functions shorten the Si–N distances by about 0.01 bohr. The differences on the equilibrium in-plane angles amount to less than 1°. The harmonic wavenumbers computed at different levels vary by less small than 10 cm^{-1}. This joins the general remarks of Werner and co-workers relative to these methods. Presently, the 6D-PESs of H_2NSi and H_2SiN will be generated using similar approach as described in Ref. 39.

B. Analytical representation of the 6D-PESs

The 6D-PESs were generated in internal coordinates (see Figure 2). Independent variables correspond to the $R_{1,2}$ (R_{HX}), R_3 (R_{XY}) elongations, the $\theta_{1,2}$ (HXY) in-plane angles and the θ out-of-plane angle, where X and Y stand for N or Si. Energies were calculated for different nuclear positions in the vicinity of the respective equilibrium geometry of the radicals. For H_2NSi, we considered geometries in the ranges $1.5 \le R_{1,2} \le 2.5$, $2.7 \le R_3 \le 3.9$, $70^\circ \le \theta_{1,2} \le 180^\circ$, and $-90^\circ \le \theta \le 90^\circ$ (in bohr and degrees), resulting in more than 1100 independent geometries. For H_2SiN, we considered less geometries (418) ranging as follows $2.4 \le R_{1,2} \le 3.2$, $2.7 \le R_3 \le 3.5$, $75^\circ \le \theta_{1,2} \le 180^\circ$, and $-30^\circ \le \theta \le 30^\circ$ (in bohr and degrees).

The constructed PESs cover energies up to $\sim$10 000 cm^{-1} above the minimum. Subsequently, the calculated energies were fitted to the following expansion, where all points are equally weighted,

$$V(R_1, R_2, R_3, \theta_1, \theta_2, \theta) = \sum_{ijklmn} c_{ijklmn} Q_1^i Q_2^j Q_3^k Q_4^l Q_5^m Q_6^n, \quad (1)$$

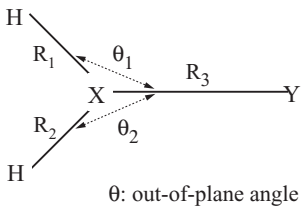

FIG. 2. Definition of the internal coordinates of H_2NSi and H_2SiN. X and Y correspond to N and Si for H_2NSi and to Si and N for H_2SiN, respectively.

with the three stretching coordinates, $Q_u = R_u\text{-}R_u^{ref}$, for u = 1–3, the two bending coordinates, $Q_u = \theta_{u\text{-}3} \text{-}\theta_{u\text{-}3}^{ref}$, for u = 4,5 ($0^\circ \leq \theta_{u\text{-}3} \leq 180^\circ$), and the out-of-plane angle, $Q_6 = \theta - \theta^{ref}$. The index "ref" denotes the reference geometry used during the fit (cf. *infra*). For H_2SiN, the exponents in the expansion were restricted to $i+j+k+l+m+n \leq 4$. For H_2NSi, the exponents in the expansion were restricted to $i+j+k+l+m+n \leq 6$. In both cases, the molecular symmetry (C_{2v}) was taken into account and only the dominant crossing terms are considered without deteriorating the quality of the fit. We optimized a total of 100 and 148 c_{ijklmn} coefficients for H_2NSi and H_2SiN, respectively, using a least squares procedure for that purposes. The root mean square of the fits was $\sim 5\ cm^{-1}$. The final values of the coefficients are available in Ref. 43.

C. Nuclear motion problem

The analytical representations of the 6D-PESs were incorporated into perturbative and variational treatments of the nuclear problem. In the perturbative approach, the 6D-PES was derived as a quartic force field in internal coordinates, which was subsequently transformed by *L*-tensor algebra into a quartic force field in dimensionless normal coordinates.[44] This procedure enables the evaluation of the spectroscopic constants up to the fourth order, using the formula developed in Refs. 45 and 46. In the variational approach, the exact calculations were performed with the fortran code ElVibRot[47] coupled with Tnum.[48,49] ElVibRot allows quantum dynamics calculations (time-dependent[50,51] or time-independent[50,52,53]) for polyatomic molecular system without built-in limitation. Tnum is used for evaluating the kinetic energy operator (KEO) numerically and exactly for a given value of the curvilinear coordinates, $\boldsymbol{q}$. The implementation of a numerical approach to the KEO has been known for many years. It was probably used for the first time in 1982 by Laane *et al.*.[54,55] Moreover, several other groups resort to similar approaches.[56–60] Our numerical implementation in Tnum is given in more details in Ref. 48.

The deformation part of the kinetic energy operator reads

$$\boldsymbol{T}_{\text{def}}(\boldsymbol{q}, \partial \boldsymbol{q}) = \sum_{i \leq j} f_2^{ij}(\boldsymbol{q}) \frac{\partial^2}{\partial q_i \partial q_j} + \sum_i f_1^i(\boldsymbol{q}) \frac{\partial}{\partial q_i} + V_e(\boldsymbol{q}),$$
$$d\tau = \rho(\boldsymbol{q}) dq_1 \cdots dq_n, \tag{2}$$

where $f_2^{ij}(\boldsymbol{q})$, $f_1^i(\boldsymbol{q})$, and $V_e(\boldsymbol{q})$ are functions of the internal coordinates. $\rho(\boldsymbol{q})$ is a weight function which enables to adapt the volume element, $d\tau$, to the vibrational basis functions. The use of the numerical approach enables to perform easily coordinate transformations such as a linear combination of the primitive internal coordinates to get symmetrized coordinates, $\boldsymbol{q}$.

In the present study, the six primitive internal coordinates (R_1, R_2, R_3, θ_1, θ_2, and θ) used to calculate the 6D-PES (see Figure 2) are symmetrized $R_\pm = 1/2\ (R_1 \pm R_2)$ and $\theta_\pm = 1/2\ (\theta_1 \pm \theta_2)$ leading to the following curvilinear coordinates, $\boldsymbol{q}$, used in dynamics: (R_+, R_-, R_3, θ_+, θ_-, and θ).

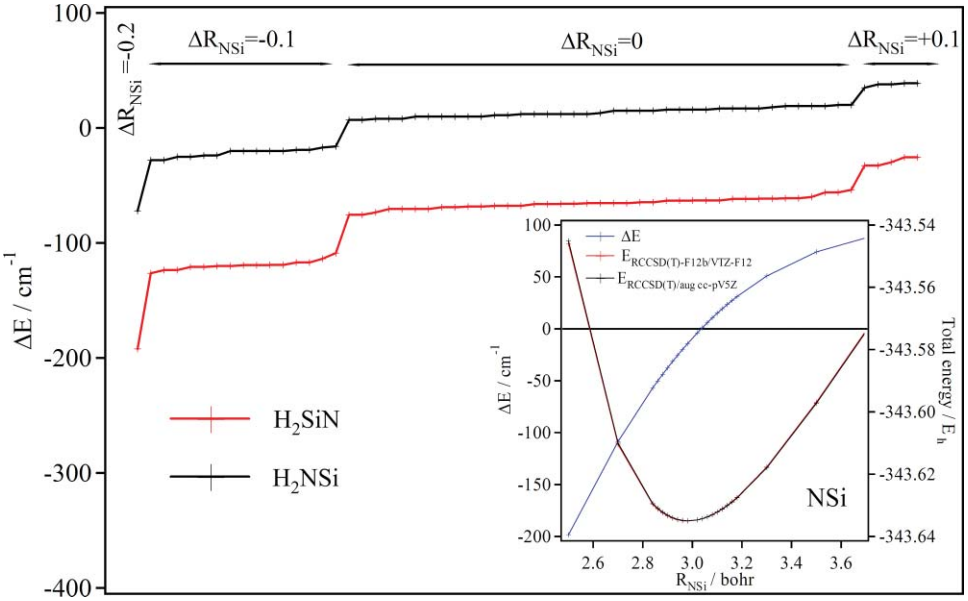

FIG. 3. Difference energy ($\Delta E = E_{RCCSD(T)\text{-}F12b/cc\text{-}pVTZ\text{-}F12} - E_{RCCSD(T)/aug\ cc\text{-}pV5Z}$, in cm^{-1}) between the total energies computed at RCCSD(T)-F12b/cc-pVTZ-F12 and RCCSD(T)/aug cc-pV5Z levels of theory for H_2NSi and H_2SiN. These energies are computed for several grid points around the equilibrium geometry where the distances are varied a maximum of ±0.2 bohr and the angles of ±10°. The inset is for similar calculations on the NSi diatomic. R_{NSi} (in bohr) corresponds to R_3 for the tetratomics and to the internuclear distance for the diatomic.

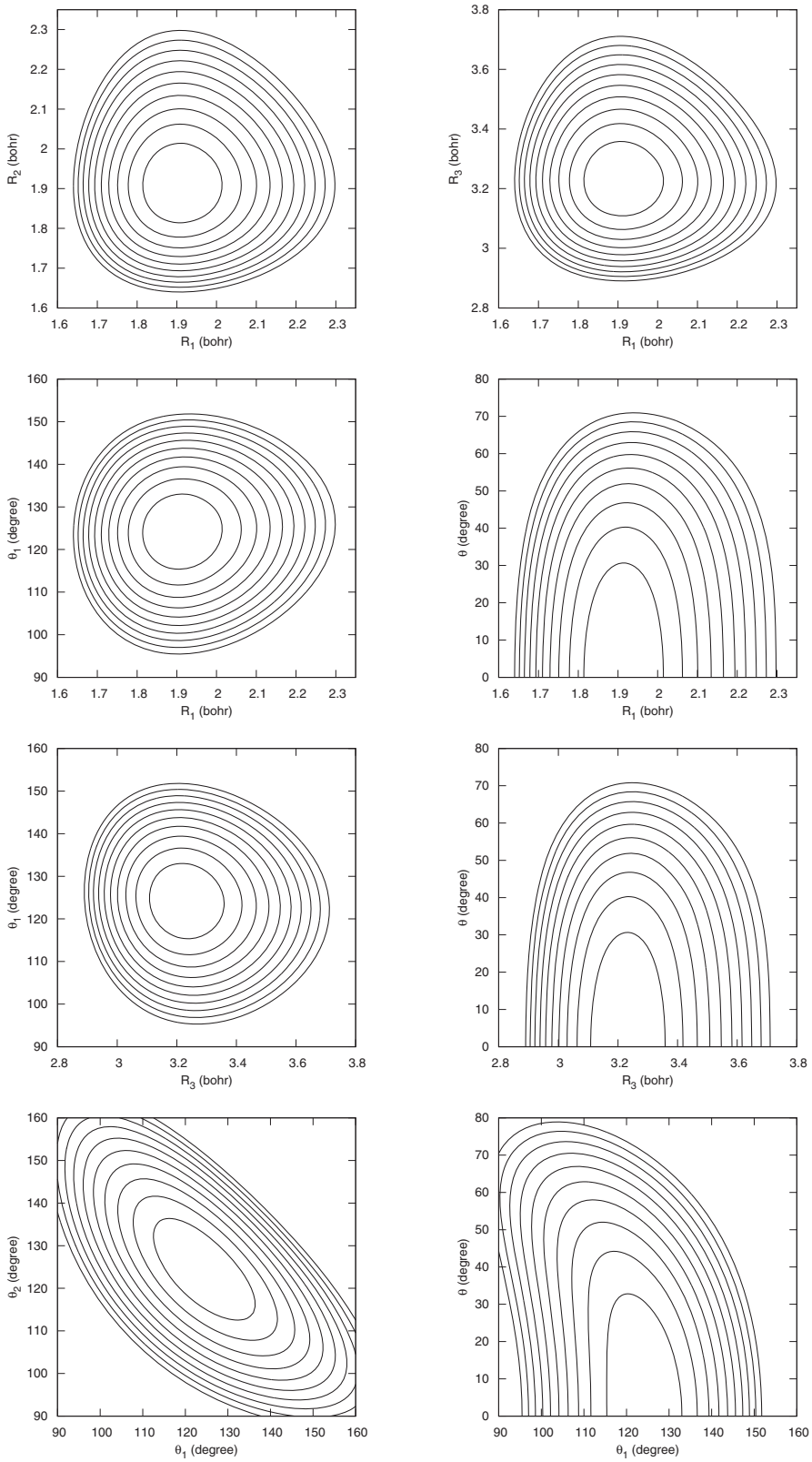

FIG. 4. Two-dimensional cuts through the RCCSD(T)-F12a/cc-pVTZ-F12 6D-PES for H_2NSi corresponding to the eight possible permutations of the internal coordinates. The other internal coordinated are set at their equilibrium values (see text). Contours are shown in steps of 500 cm^{-1}.

For each degree-of-freedom, a 1D-harmonic oscillators (HO) basis set is used. These basis functions are contracted to form two 3D-basis sets. The first one and the second one are associated to the three distances and the three angles, respectively. This contraction enables to obtain a compact description of the eigenstates. For each 3D-basis set, about one hundred basis-functions are used. The integration procedure is performed using a direct product of Gauss-Hermite quadrature grids and the diagonalization is performed using a Block-Davidson scheme without storing the full Hamiltonian matrix.

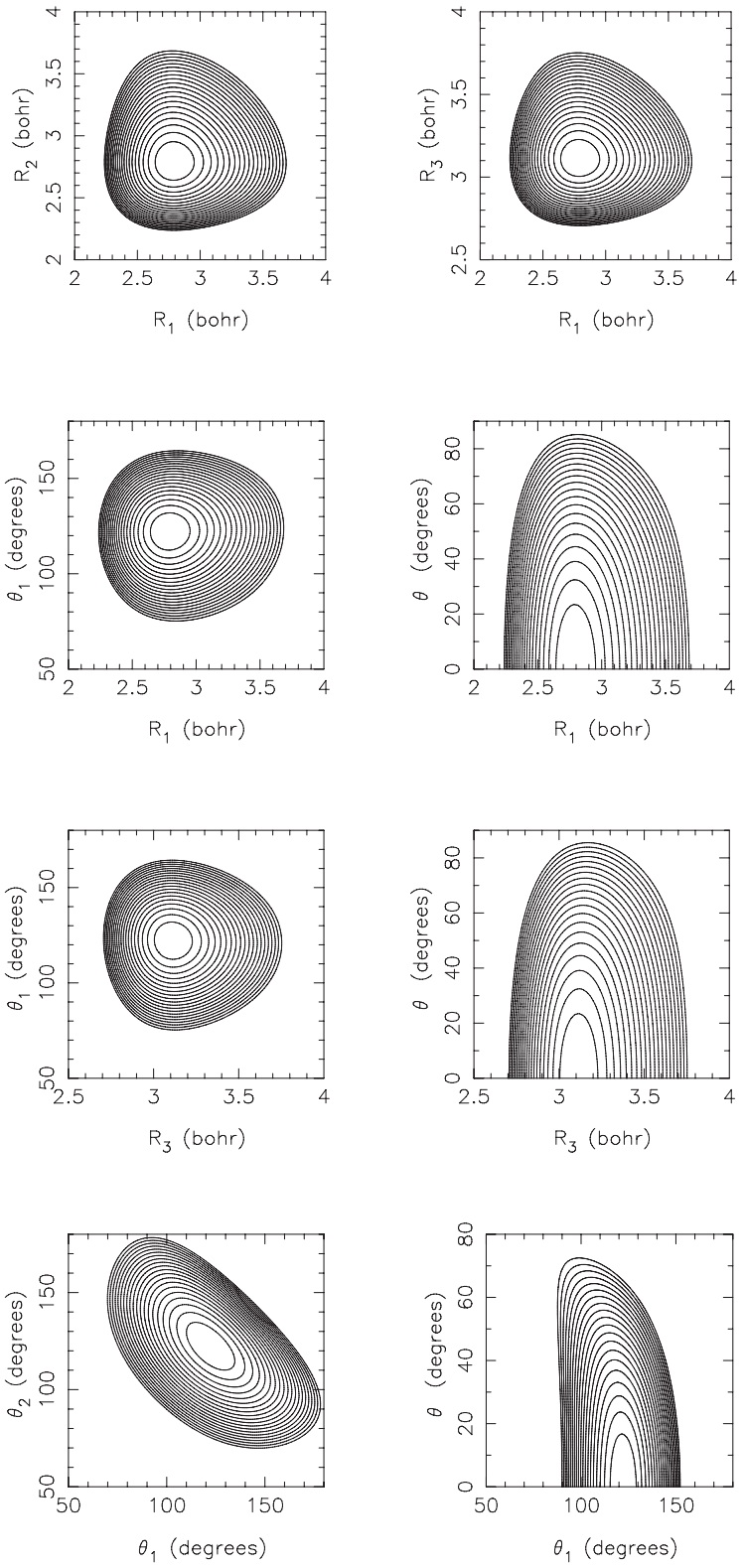

FIG. 5. Two-dimensional cuts through the RCCSD(T)-F12a/cc-pVTZ-F12 6D-PES for H_2SiN corresponding to the eight possible permutations of the internal coordinates. The other internal coordinates are set at their equilibrium values (see text). Contours are shown in steps of 500 cm^{-1} except the θ_1/θ cut for which the step is 250 cm^{-1}.

This scheme has been described in detail by Ribeiro *et al.*[61] and also by others.[62,63]

Our procedure enables to get the vibrational eigenstates of H_2SiN and H_2NSi (J = 0) up to 4000 cm^{-1}. The energy levels of fundamental transitions are converged within 0.1 cm^{-1}. For some overtones or combination modes, the convergence is higher up to 2 cm^{-1}. Such levels are denoted as "not fully converged" in the following tables. The accuracy

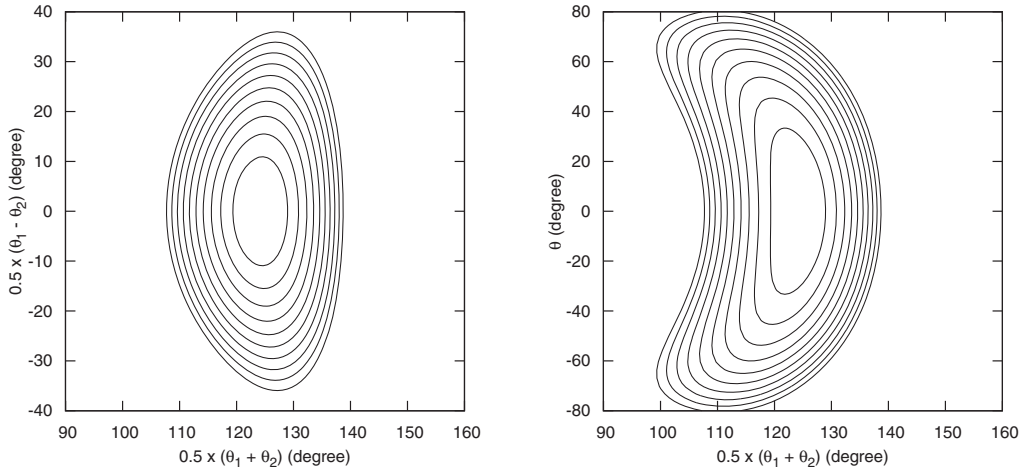

FIG. 6. Contour plots of the 2D cuts of the RCCSD(T)-F12a/cc-pVTZ-F12 6D-PES of H_2NSi along the symmetric ($\theta_+ = 1/2\ (\theta_1 + \theta_2)$) and antisymmetric bending ($\theta_- = 1/2\ (\theta_1 - \theta_2)$) coordinates (left), and the symmetric bending coordinate ($\theta_+ = 1/2\ (\theta_1 + \theta_2)$), and the out-of-plane angle (θ) (right). The step between the contours is 500 cm^{-1}.

of the variational energy levels is linked to the potential energy surface precision. It is expected to be around 20 cm^{-1} according to similar works.[64]

III. RESULTS AND DISCUSSION

In the literature, RCCSD(T)-F12b/cc-pVTZ-F12 gives total energies close to those calculated using RCCSD(T)/aug cc-pV5Z and with a small constant shift. For H_2NSi, H_2SiN, and the NSi diatomic, Figure 3 displays the evolution of the difference energies (ΔE), which corresponds to $E_{RCCSD(T)\text{-}F12b/cc\text{-}pVTZ\text{-}F12} - E_{RCCSD(T)\ /aug\ cc\text{-}pV5Z}$.

This figure shows that for H_2NSi and SiN molecular systems, ΔE is close to zero and within the expected error bars for the R_{NSI} distances close to equilibrium (R_{NSI} for NSi diatomic and R_3 for the tetratomics). In contrast, for all the energies of H_2SiN, a systematic shift of $\sim$60 cm^{-1} is found together with an additional systematic shift to lower energies of $E_{RCCSD(T)\text{-}F12b/cc\text{-}pVTZ\text{-}F12}$ with respect to $E_{RCCSD(T)\ /aug\ cc\text{-}pV5Z}$ for $\Delta R_{NSi} < 0$. Such differences seem to be reduced for $\Delta R_{NSi} > 0$. The inset in Figure 3 shows a similar tendency for the SiN diatomic. These effects remain small and the general shape of the 6D-PESs is similar, especially, for the RCCSD(T)-F12a/cc-pVTZ-F12 and RCCSD(T)-F12b/cc-pVTZ-F12 ones. For more clarity of the manuscript, we will discuss only the RCCSD(T)-F12a/cc-pVTZ-F12 6D-PESs (Figures 4 and 5). Therefore, this effect will not affect strongly the rovibrational energies computed for H_2NSi at all levels of theory whereas we expect some differences for H_2SiN (cf. *infra*).

TABLE I. Harmonic wavenumbers (ω_i), rotational constants (A_e, B_e, C_e), first order centrifugal distortion constants (D_J, D_{JK}, D_K), A-reduction distortion constants (Δ_J, Δ_{JK}, Δ_K, δ_J, δ_K), and vibration-rotation constants (α_i) of H_2NSi and H_2SiN computed with RCCSD(T)-F12a/cc-pVTZ-F12. All values are in cm^{-1}.

Spectroscopic parameters	H_2NSi	H_2SiN	Spectroscopic parameters	H_2NSi	H_2SiN
ω_1	3533.1	2263.5	α_1^A	0.2073	0.0736
ω_2	1584.3	1035.0	α_2^A	–0.2924	–0.0173
ω_3	870.0	923.1	α_3^A	0.0068	–0.0699
ω_4	571.9	542.6	α_4^A	1.0549	–1.0134
ω_5	3625.7	2295.0	α_5^A	0.1168	0.05277
ω_6	734.9	508.8	α_6^A	–1.3573	0.9655
A_e	12.0009	5.3759	α_1^B	0.00032	0.00051
B_e	0.5140	0.5871	α_2^B	0.00016	0.00362
C_e	0.4929	0.5293	α_3^B	0.00359	–0.00067
D_J	0.6546×10^{-6}	0.6677×10^{-6}	α_4^B	0.00382	0.00407
D_{JK}	0.2861×10^{-4}	0.3303×10^{-4}	α_5^B	0.00059	0.00071
D_K	0.1213×10^{-2}	0.2501×10^{-3}	α_6^B	–0.00152	–0.00341
Δ_J	0.6557×10^{-6}	0.6760×10^{-6}	α_1^C	0.00063	0.00111
Δ_{JK}	0.2860×10^{-4}	0.3298×10^{-4}	α_2^C	0.00129	0.00362
Δ_K	0.1213×10^{-2}	0.2502×10^{-3}	α_3^C	0.00303	0.00144
δ_J	0.2819×10^{-7}	0.7486×10^{-7}	α_4^C	0.00153	0.00008
δ_K	0.1708×10^{-4}	0.1948×10^{-4}	α_5^C	0.00062	0.00092
			α_6^C	0.00067	0.00044

A. Description of the 6D-PESs

Figures 4 and 5 depict the 2D cuts through our 6D PESs of the H_2NSi and H_2SiN radicals along two of the internal coordinates, the remaining internal coordinates being set to their equilibrium values (see below). For each isomer, the cuts display a unique minimum, corresponding to the radical equilibrium geometry of interest here.

For both molecules, our cuts present similar shapes as those known for formaldehyde type molecules,[65,66] where a strong coupling is observable for the θ_1/θ_2 cuts. For the other cuts, Figures 4 and 5 reveal that the stretches and the in-plane angles are slightly coupled. These couplings are confirmed by the decomposition of the normal modes into the internal coordinates.

Let us concentrate now on the 2D contour plots through the out-of-plane angle (θ) and the in-plane angle (θ_1) of Figures 4 and 5. These plots show that our 6D-PESs are flat along the out-of-plane angle, especially for the H_2NSi isomer where the contour at 500 cm^{-1} extends till $\theta \sim 30°$. Such behavior constrained us to add some specific c_{ijklmn} coefficient cross terms during the fitting procedure of the *ab initio* energies for more flexibility of corresponding analytic representations. This specific behavior results on couplings between the modes involving θ_1/θ_2 and θ. For illustration, Figure 6 displays the 2D contour plots of the 6D- PES of H_2NSi along the out-of-plane, the symmetric bending, and antisymmetric bending coordinates. We notice the flatness of this 6D-PES along the corresponding symmetrized coordinates. In addition, one can clearly see that the potential energy valleys are not parallel to the *y*-axis signature of the occurrence of additional couplings between these modes. This is not fully accounted for in perturbation theory since the harmonic approximation is not appropriate to provide accurately the spectrum for such vibrational modes. As noticed in Ref. 17, only a full 6D variational approach on a full 6D-PES similar to the one performed here, should be used to get the vibrational spectrum of these molecular species. This was already observed for other molecular systems, such as N_2CO^+, N_4^+, N_2HAr^+, and $HNNH^+$.[62,67–69]

B. Spectroscopic parameters

For H_2NSi (isomer I), our equilibrium geometry is: R_{NH} = 1.009 Å, R_{SiN} = 1.707 Å and the in-plane HNSi angle = 124.25°. For H_2SiN (isomer III), we compute: R_{SiH} = 1.475 Å, R_{SiN} = 1.646 Å, and HSiN = 122.25°. These equilibrium geometries are deduced from our RCCSD(T)-F12a/cc-pVTZ-F12 6D-PESs. They coincide with those obtained at the RCCSD(T)/aug cc-pV5Z and RCCSD(T)-F12b/cc-pVTZ-F12 levels of theory. When we compare to the parameters given in Ref. 17, one can find that the present equilibrium geometries are close to those computed for isomer I using RCCSD(T)/cc-pVQZ and RCCSD(T)/aug cc-pVQZ, whereas, for isomer III, the stretchings are shorter by ~0.15–0.12 Å and the angles are smaller by ~5°. The present treatment should be viewed as more accurate since it takes into account larger electron correlation amount. Therefore, we recommend the equilibrium geometries quoted here.

Both molecules are asymmetric type rotor (near prolate symmetric top; κ close to –1). Table I lists their equilibrium rotational constants (A_e, B_e, and C_e), their first order centrifugal distortion (D_J, D_{JK}, D_K) terms, the quartic centrifugal-distortion constants within the case of Watson's A-reduction (Δ_J, Δ_{JK}, Δ_K, δ_J, δ_K), and the vibration-rotation constants (α_i). These values are obtained from the quartic force field in dimensionless coordinates.[45,46,64] These quantities represent predictions and should be accurate enough to be helpful for the attribution of the rotationally resolved experimental spectra of these radicals whenever measured.

C. Variationally determined vibrational spectra of H_2NSi and of H_2SiN

As for formaldehyde, H_2NSi and H_2SiN radicals have six vibrational modes: symmetric HX stretch, XY stretch, and symmetric HXY in-plane bending, ν_{1-3} (a_1), one out-of-plane, ν_4 (b_1) and antisymmetric HX stretch and antisymmetric HXY in-plane bending, $\nu_{5,6}$ (b_2). Tables II and III list their variationally computed anharmonic wavenumbers (ν_i).

For H_2NSi, we give only the data derived from the RCCSD(T)-F12a/cc-pVTZ-F12 potential since the RCCSD(T)-F12b/cc-pVTZ-F12 and the standard RCCSD(T)/aug cc-pV5Z 6D PESs lead to similar results (see Figure 3). For this radical, the RCCSD(T)-F12a/cc-pVTZ-F12 variationally determined fundamentals have been found to be: (in cm^{-1}): ν_1 (NH symmetric stretch) = 3368.3, ν_2 (symmetric bending) = 1558.9, ν_3 (SiN stretching) = 857.5, ν_4 (out-of-plane) = 560.8, ν_5 (antisymmetric NH stretching) = 3441.3 and ν_6 (antisymmetric bending) = 725.3,

TABLE II. Variational vibrational energies (in cm^{-1}) of H_2NSi and their tentative assignment. These data are derived from the RCCSD(T)-F12a/ cc-pVTZ-F12 6D-PES. The fundamentals are given in bold characters. The number of digits corresponds to the numerical convergence precision on the energy.

(v_1,v_2,v_3,v_4,v_5,v_6)	Energy/cm^{-1}
(0,0,0,0,0,0)	0.0[a]
(0,0,0,1,0,0)	**560.8**
(0,0,0,0,0,1)	**725.3**
(0,0,1,0,0,0)	**857.5**
(0,0,0,2,0,0)	1112.2[b]
(0,0,0,1,0,1)	1295.9
(0,0,1,1,0,0)	1410.3
(0,0,0,0,0,2)	1440.9
(0,1,0,0,0,0)	**1558.9**
(0,0,1,0,0,1)	1582.7
(0,0,2,0,0,0)	1707.1
(0,1,0,1,0,0)	2146.5[b]
(0,1,0,0,0,1)	2288.1
(0,1,1,0,0,0)	2413.0
(0,2,0,0,0,0)	3101.7[b]
(1,0,0,0,0,0)	**3368.3**
(0,0,0,0,1,0)	**3441.3**
(1,0,0,1,0,0)	3917.2
(0,0,0,1,1,0)	3981.7

[a]Zero point vibrational energy (ZPE) = 5377.37 cm^{-1}.
[b]Not fully converged. See text.

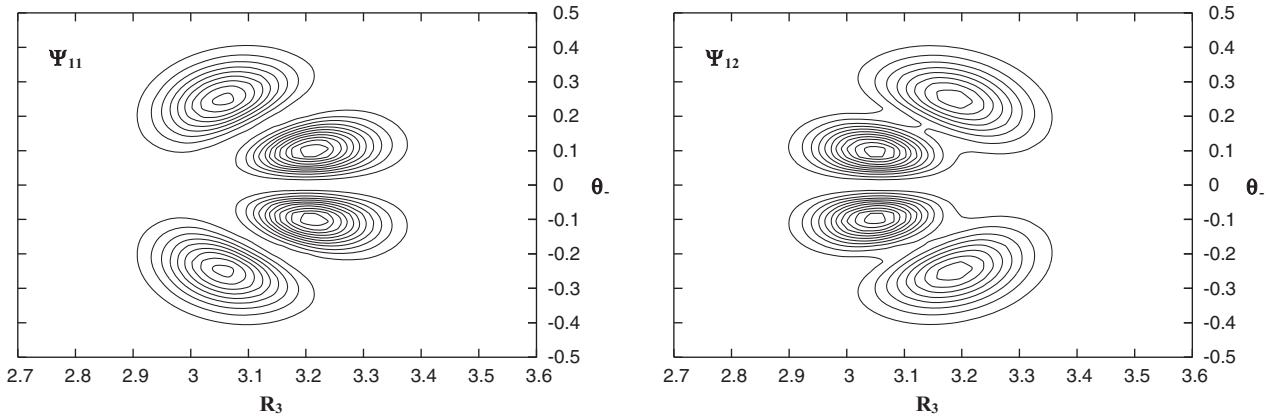

FIG. 7. The 2D-reduced density along the antisymmetric bending ($\theta_- = 1/2\ (\theta_1 - \theta_2)$) coordinate and the SiN stretch (R_3) of the 11th and the 12th resonant-states of H_2SiN at 1502 and 1514 cm^{-1}, above the zero point vibrational energy with the RCCSD(T)-F12a/cc-pVTZ-F12 potential. The zero-order states involved in these resonances are the (0,0,1,0,0,1) and (0,0,0,0,0,3). See text for more details.

respectively (cf. Table II). Table III also gives the tentatively assigned spectrum for the main set of the vibrational levels up to ~4000 cm^{-1} above the zero point vibrational energy. For that purpose we examinated the decomposition of the rovibrational wavefunctions on the harmonic oscillator basis set.

TABLE III. Variational vibrational energies (in cm^{-1}) of H_2SiN and their tentative assignment. These data are derived from our RCCSD(T)/aug-cc-pV5Z, RCCSD(T)-F12a/cc-pVTZ-F12, and RCCSD(T)-F12b/cc-pVTZ-F12 6D-PESs. We give the fundamentals in bold characters. The number of digits corresponds to the numerical convergence precision on the energy.

(v_1,v_2,v_3,v_4,v_5,v_6)	RCCSD(T)/aug-cc-pV5Z	RCCSD(T)-F12a/cc-pVTZ-F12	RCCSD(T)-F12b/cc-pVTZ-F12
(0,0,0,0,0,0)	0.0[a]	0.0[b]	0.0 [c]
(0,0,0,0,0,1)	**488.3**	**501.3**	**502.1**
(0,0,0,1,0,0)	**534.8**	**531.3**	**531.0**
(0,0,1,0,0,0)	**894.7**	**899.6**	**900.0**
(0,0,0,0,0,2)	981.8	1002.3	1003.7
(0,1,0,0,0,0)	**1007.4**	**1010.0**	**1010.9**
(0,0,0,1,0,1)	1030.7	1040.5	1041.1
(0,0,0,2,0,0)	1079.7	1067.4	1067.3
(0,0,1,0,0,1)	1379.8	1395.7	1396.9
(0,0,1,1,0,0)	1414.9	1416.0	1416.1
(0,0,0,0,0,3)	1480.1	1502.0 [d]	1504.0 [d]
(0,0,1,0,0,1)	1494.5	1514.2[d]	1516.0[d]
(0,1,0,1,0,0)	1525.9	1521.1	1521.5
(0,0,2,0,0,0)	1784.3	1794.0	1794.7
(0,1,1,0,0,0)	1892.0	1894.7	1894.4
(0,2,0,0,0,0)	2001.6	1999.1	2001.0
(1,0,0,0,0,0)	**2185.9**	**2194.0**	**2193.9**
(0,0,0,0,1,0)	**2210.1**	**2210.2**	**2210.0**
(1,0,0,0,0,1)	2665.7	2688.0	2688.7
(0,0,0,0,1,1)	2688.6	2700.6	2701.3
(1,0,0,1,0,0)	2715.2 [e]	2725.2	2725.0
(0,0,0,1,1,0)	2739.0	2731.6	2731.3
(1,0,1,0,0,0)	3071.0	3086.8	3087.1
(0,0,1,0,1,0)	3094.3	3100.5	3100.7

[a]Zero point vibrational energy (ZPE) = 3608.04 cm^{-1}.
[b]Zero point vibrational energy = 3739.95 cm^{-1}.
[c]Zero point vibrational energy = 3740.77 cm^{-1}.
[d]Resonant-states from the zero-order states, (0,0,0,0,0,3) and (0,0,1,0,0,1).
[e]Not fully converged. See text.

For H_2SiN, we list in Table III the spectra obtained using the three *ab initio* methods for comparison. Close examination of Table III reveals that some fundamentals present 3–13 cm^{-1} differences depending on the 6D potential used in the nuclear motion treatment. This is most likely related to the total energies evolutions computed over the grid for this isomer, especially along the SiN intramolecular distance (cf. Figure 3). For the H_2SiN molecule, the RCCSD(T)-F12a/cc-pVTZ-F12 variationally determined fundamentals are: ν_1 (symmetric SiH stretching) = 2194.0, ν_2 (SiN stretching) = 1010.0, ν_3 = 899.6, ν_4 = 531.3, ν_5 = 2210.2, and ν_6 = 501.3 (all values are in cm^{-1}). Moreover, the analysis of the vibrational wavefunctions reveals the occurrence of some resonances when using the RCCSD(T)-F12a/b potentials. Indeed, the transitions ν_3 and $2\nu_6$ are almost degenerated for the RCCSD(T)-F12a/b potentials. Therefore, resonances may appear for polyads (such $2\nu_3 + \nu_6 = p$) with the zero-order states (0,0,ν_3,0,0,ν_6). For p = 2, the resonance is weak (5th and 6th states). However, for p = 3, a strong resonance occurs between the zero-order states (0,0,1,0,0,1) and (0,0,0,0,0,3) (both of them are of b_2 symmetry) to give the 11th and the 12th states at 1502 cm^{-1} and 1514 cm^{-1}, respectively. This resonance is clearly visible in Figure 7 in which the 2D-reduced density of both eigenstates is plotted as a function of the symmetrized coordinates θ_- and R_3, associated with the antisymmetric bend and SiN stretching mode, respectively. Such accidental resonances are very sensitive on the quality of the 6D-PES and they were not located using the RCCSD(T)/aug cc-pV5Z potential.

IV. CONCLUSION

For the H_2NSi and H_2SiN isomers, we computed the 6D-PESs of their electronic ground state using standard RCCSD(T) coupled cluster and the newly developed RCCSD(T)-F12 methods. After variational treatments of the nuclear motions using these PESs, the vibrational spectra of these radicals are deduced up to ~4000 cm^{-1} above the zero point vibrational energy. The RCCSD(T)-F12(a/b)/cc-

pVTZ-F12 approaches lead *a priori* to equivalent results (within the spectroscopic accuracy) as those obtained using the standard coupled cluster approaches and a larger basis set (at least of aug-cc-pV5Z quality) with strong reductions of CPU time and of disk occupancy for a single point electronic calculation. As already pointed out in previous benchmarking studies,[39–42,70,71] these explicitly correlated methods represent a compromise for good description of the PESs and computation cost. It is, therefore, recommended for full dimensional PES generation of polyatomic molecular systems. Nevertheless, the slight differences observed in the case of H_2SiN suggest that special cares need *a priori* to be taken when considering molecules bearing heavy atoms such as Si.

ACKNOWLEDGMENTS

L.J. thanks the Centre National de la Recherche Scientifique (CNRS, France) for financial support. M.L.S. acknowledges the *MICINN* (SPAIN) for the Grant No. AYA2008–00446.

[1]D. W. Hughes, in *Cosmic Dust*, edited by J. A. M. McDonnell (Wiley, New York 1978), p. 123.
[2]J. M. C. Plane, Chem. Rev. **103**, 4963 (2003).
[3]C. Koeberl and E. H. Hagen, Geochim. Cosmochim. Acta **53**, 937 (1989).
[4]T. Vondrak, J. M. C. Plane, S. Broadley, and D. Janches, Atmos. Chem. Phys. Discuss. **8**, 14557 (2008).
[5]J. C. Gómez Martín, M. A. Blitz, and J. M. C. Plane, Phys. Chem. Chem. Phys. **11**, 671 (2009).
[6]E. E. Ferguson, D. W. Fahey, F. C. Fehsenfeld, and D. L. Albritton, Planet. Space Sci. **29**, 307 (1981).
[7]B. E. Turner, Astrophys. J. **388**, L35 (1992).
[8]M. J. Kushner, J. Appl. Phys. **71**, 4173 (1992).
[9]T. Ito, I. Kato, T. Nozaki, T. Nakamura, and H. Ishikawa, Appl. Phys. Lett. **38**, 370 (1981).
[10]F. Bozso and P. Avouris, Phys. Rev. Lett. **57**, 1185 (1986).
[11]R. Urmi and F. F. J. Martin, J. Chem. Phys. **93**, 5709 (1990).
[12]G. A. Brown, W. C. Robinette, Jr., and H. G. Carlson, J. Electrochem. Soc. **115**, 948 (1968).
[13]G. T. Burns and G. Chandra, J. Am. Ceram. Soc. **72**, 333 (1989).
[14]F. L. Riley, J. Am. Ceram. Soc. **83**, 245 (2000).
[15]W. Zhu, D. Neumayer, V. Perebeinos, and P. Avouris, Nano Lett. **10**, 3572 (2010).
[16]H. L. Chen, C. W. Wu, and J. J. Ho, J. Phys. Chem. A **110**, 8893 (2006).
[17]M. Hochlaf, G. Chambaud, and M. L. Senent, Mol. Phys. **108**, 1277 (2010).
[18]N. Goldberg, J. Hrusak, M. Iraqi, and H. Schwarz, J. Phys. Chem. **97**, 10687 (1993).
[19]R. Damrauer, M. Krempp, and R. A. J. O'Hair, J. Am. Chem. Soc. **115**, 1998 (1993)
[20]W.-K. Chen, I-Ch. Lu, Ch. Chaudhuri, W.-J. Huang, and S.-H. Lee, J. Phys. Chem. A **112**, 8479 (2008).
[21]I.-C. Lu, W.-K. Chen, C. Chaudhuri, W.-J. Huang, J. J. Lin, and S.-H. Lee, J. Chem. Phys. **129**, 174304 (2008).
[22]S. Wlodek and D. K. Bohme, J. Am. Chem. Soc. **110**, 2396 (1988).
[23]S. J. Branko, J. Mol. Struct.: THEOCHEM **455**, 77 (1998).
[24]O. Parisel, M. Hanus, and Y. Ellinger, Chem. Phys. **212**, 331 (1996).
[25]O. Parisel, M. Hanus, and Y. Ellinger, J. Phys. Chem. **100**, 2926 (1996).
[26]O. Parisel, M. Hanus, and Y. Ellinger, J. Chem. Phys. **104**, 1979 (1996).
[27]O. Parisel, M. Hanus, and Y. Ellinger, J. Phys. Chem. A **101**, 299 (1999) and references therein.
[28]H.-J. Werner, P. J. Knowles, G. Knizia, F. R. Manby, M. Schütz *et al.*; MOLPRO, a package of *ab initio* programs, version 2010.1, see http://www.molpro.net.
[29]P. J. Knowles, C. Hampel, and H.-J. Werner, J. Chem. Phys. **99**, 5219 (1993); **112**, 3106 (2000) (Erratum).
[30]K. Raghavachari, G. W. Trucks, J. A. Pople, and M. Head-Gordon, Chem. Phys. Lett. **157**, 479 (1989).
[31]H. J. Werner, T. B. Adler, and F. R. Manby, J. Chem. Phys. **126**, 164102 (2007).
[32]T. B. Adler, G. Knizia, and H.-J. Werner, J. Chem. Phys. **127**, 221106 (2007).
[33]K. A. Peterson, T. B. Adler, and H-J. Werner, J. Chem. Phys. **128**, 084102 (2008).
[34]T. H. Dunning, Jr., J. Chem. Phys. **90**, 1007 (1989).
[35]D. E. Woon and T. H. Dunning, Jr., J. Chem. Phys. **98**, 1358 (1993).
[36]F. Weigend, Phys. Chem. Chem. Phys. **4**, 4285 (2002).
[37]C. Hättig, Phys. Chem. Chem. Phys. **7**, 59 (2005).
[38]W. Klopper, Mol. Phys. **99**, 481 (2001).
[39]V. Brites and M. Hochlaf, J. Phys. Chem. A **113**, 11107 (2009), and references therein.
[40]F. Lique, J. Klos, and M. Hochlaf, Phys. Chem. Chem. Phys. **12**, 15672 (2010).
[41]G. Rauhut, G. Knizia, and H.-J. Werner, J. Chem. Phys. **130**, 054105 (2009).
[42]X. Huang, E. F. Valeev, and T. J. Lee, J. Chem. Phys. **133**, 244108 (2010).
[43]See supplementary material at http://dx.doi.org/10.1063/1.3624563 for the expansions of the PESs and the equilibrium geometries and the harmonic frequencies of H_2SiN and H_2NSi at different *ab initio* levels.
[44]M. Hochlaf, Trends Chem. Phys. **12**, 1 (2005).
[45]D. Papousek and M. R. Aliev, in *Molecular Vibrational-Rotational Spectra* (Elsevier, New York, 1982).
[46]I. M. Mills, in *Molecular Spectroscopy: Modern Research*, edited by K. N. Rao and C. W. Mathews (Academic, New York, 1972).
[47]D. Lauvergnat, ElVibRot: quantum dynamics code. http://www.lcp.u-psud.fr/Pageperso/lauvergnat/perso/.
[48]D. Lauvergnat and A. Nauts, J. Chem. Phys. **116**, 8560 (2002).
[49]D. Lauvergnat, Tnum: Numerical kinetic energy operator code. http://www.lcp.u-psud.fr/Pageperso/lauvergnat/perso/.
[50]L. Bomble, D. Lauvergnat, F. Remacle, and M. Desouter-Lecomte, J. Chem. Phys. **128**, 064110 (2008).
[51]D. Lauvergnat, S. Blasco, X. Chapuisat, and A. Nauts, J. Chem. Phys. **126**, 204103 (2007).
[52]D. Lauvergnat and A. Nauts, Chem. Phys. **305**, 105, (2004).
[53]S. Blasco and D. Lauvergnat, Chem. Phys. Lett. **373**, 344 (2003).
[54]J. Laane, M. A. Harthcock, P. M. Killough, L. E. Bauman, and J. M. Cooke, J. Mol. Spectrosc. **91**, 286 (1982).
[55]M. A. Harthcock and J. Laane, J. Mol. Spectrosc. **91**, 300 (1982).
[56]M. L. Senent and Y. G. Smeyers, J. Chem. Phys. **105**, 2789 (1996).
[57]C. Muñoz-Caro and A. Niño, QCPE Bull. **13**, 4 (1993).
[58]M. L. Senent, Chem. Phys. Lett. **296**, 299 (1998).
[59]D. J. Rush and K. B. Wiberg, J. Phys. Chem. A **101**, 3143 (1997).
[60]E. Mátyus, G. Czakó, and A. G. Császár, J. Chem. Phys. **130**, 134112 (2009).
[61]F. Ribeiro, C. Iung, and C. Leforestier, J. Chem. Phys. **123**, 054106 (2005).
[62]D. Lauvergnat and M. Hochlaf, J. Chem. Phys. **130**, 224312 (2009).
[63]Y. Scribano, D. Lauvergnat, and D. M. Benoit, J. Chem. Phys. **133**, 094103 (2010).
[64]F. Richter, M. Hochlaf, P. Rosmus, F. Gatti, and H.-D. Meyer, J. Chem. Phys. **120**, 1306 (2004).
[65]J. M. L. Martin, T. J. Lee, and P. R. Taylor, J. Mol. Spectrosc. **160**, 105 (1993).
[66]N. Lakin, M. Hochlaf, G. Chambaud, and P. Rosmus, J. Chem. Phys. **115**, 3664 (2001).
[67]M. Hochlaf, C. Léonard, E. E. Ferguson, P. Rosmus, E. A. Reinsch, S. Carter, and N. C. Handy, J. Chem. Phys. **111**, 4948 (1999).
[68]C. Léonard, P. Rosmus, S. Carter, and N. C. Handy, J. Phys. Chem. A **103**, 1846 (1999).
[69]V. Brites, O. Dopfer, and M. Hochlaf, J. Phys. Chem. A **112**, 11283 (2008).
[70]N. Inostroza and M. L. Senent, J. Chem. Phys. **133**, 184107 (2010).
[71]M. L. Senent and R. Dominguez-Gomez, Chem. Phys. Lett. **501**, 25 (2010).